Journal of Applied Analysis and Computation
Volume 4, Number 4, November 2014
Website:http://jaac-online.com/
pp. 389–403

THE STUDY OF HEAT AND MASS TRANSFER IN A VISCO ELASTIC FLUID DUE TO A CONTINUOUS STRETCHING SURFACE USING HOMOTOPY ANALYSIS METHOD

Rajeswari Seshadri[1,†] and Shankar Rao Munjam[1]

Abstract In this paper, an approximate analytical solution is derived for the flow velocity and temperature due to the laminar, two-dimensional flow of non-Newtonian incompressible visco elastic fluid due to a continuous stretching surface. The surface is stretched with a velocity proportional to the distance x along the surface. The surface is assumed to have either power-law heat flux or power-law temperature distribution. The presence of source/sink and the effect of uniform suction and injection on the flow are considered for analysis. An approximate analytical solution has been obtained using Homotopy Analysis Method(HAM) for various values of visco elastic parameter, suction and injection rates. Optimal values of the convergence control parameters are computed for the flow variables. It was found that the computational time required for averaged residual error calculation is very very small compared to the computation time of exact squared residual errors. The effect of mass transfer parameter, visco elastic parameter, source/sink parameter and the power law index on flow variables such as velocity, temperature profiles, shear stress, heat and mass transfer rates are discussed.

Keywords Two-dimensional flow, HAM solution, viscoelastic, stretching surface.

MSC(2000) 76M25, 76N20, 76W05, 80A20.

1. Introduction

The heat and mass transfer study over a continuously stretching surface is one of the important areas of current research. This finds its application over a broad spectrum of Science and Engineering disciplines, especially in the field of chemical engineering.

Many chemical engineering processes like glass blowing and polymer extrusion involve cooling of a molten liquid being stretched into a cooling system [2]. As polymer is a flexible, the filament surface may stretch during the course of blowing and hence the surface velocity deviates from being uniform [5].

In such processes the fluid mechanical properties of the final product would mainly depend on the cooling liquid used and the rate of stretching. Some of the polymer fluids such as Polyethylene oxide, poly-isobutylene solution in cetane are necessarily non Newtonian fluids. An utmost care has to be taken to control the rate

[†]the corresponding author. Email address: oviaraji@yahoo.com(R. Seshadri)
[1]Department of Mathematics, Ramanujan School of Mathematical Sciences, Pondicherry University, Pondicherry-605014, India

of cooling liquids it is stretched to get the end product with desired characteristics. Care has to be taken to avoid rapid stretching that results in sudden solidification thereby destroying the properties expected for the outcome.

The problem addressed here is a fundamental one that arises in many practical situations. To name some of them, drawing, annealing and tinning of copper wires, continuous stretching, rolling and manufacturing of plastic films and artificial fibres, materials manufactured by extrusion process and heat treated materials traveling between a feed roll and windup rolls or on conveyer belts, glass blowing, crystal growing, paper production [24].

Sakiadis [27] was the first to study the boundary layer flow over a continuous moving surface in an ambient fluid. Due to the entrainment of ambient fluid, this boundary layer flow is quite different from the boundary layer flow over a stretching semi-infinite flat plate in a fluid with a free stream.

Erickson et al. [7] extended this problem to study the temperature distribution of the stretching surface in the boundary layer when the sheet is maintained at a constant temperature with suction or injection. Crane [6] obtained an elegant analytical solution to the boundary layer equations for the problem of steady two dimensional flows due to a stretching surface in a quiescent incompressible fluid.

Following that, several solution procedures such as analytical solutions, closed form solution, asymptotic solutions and numerical solutions on stretching surfaces for various cases of flow are available in the literature. The solution analysis for stretching surfaces in terms of finding approximate analytical solution procedure recently pick up popularity with the help of the Homotopy Analysis Method (HAM) first described by Liao [12]. The advantage of HAM is its independence on small physical parameters such as convergence control parameter and auxiliary parameters [30]. HAM can control and adjust the convergence region and rate of the homotopy solutions [12] and [11].

To increase the efficiency of HAM, many authors have considered several analysis. Liao [16] and Marinca et al. [18], Zhao et al. [31] and Araghi et al. [3] have suggested an optimal HAM, optimal homotopy asymptotic method and modified HAM which improves the solution by reducing the CPU time as well as minimizing the residual errors.

The two-dimensional, magnetohydrodynamic non-Newtonian incompressible flow due to a stretching sheet was studied using HAM by Liao [13]. Following this, several other studies using HAM are available in the open literature Liao [15], [14] and Abbasbandy [1] including one or more parameters such as magnetic effect, injection or suction.

Recently, Misra et al. [20] studied the steady MHD flow of a visco-elastic fluid in a parallel channel in an uniform transverse magnetic field using perturbation analysis and numerical methods. Raftari et al. [23] obtained the solution of the MHD viscoelastic fluid flow and heat transfer in a channel with a stretching wall using HAM. More researchers, Sajid et al. [26] and Hayat et al. [10], Shehzad et al. [29], [28] and Chen and Char [5] have considered the heat transfer problem of viscoelastic fluid over a continuous stretching surface. Recently Prasad et al. [22] have studied thermal radiation effects on viscoelastic fluid flow and heat transfer due to a stretching sheet using numerical method such as Runge - Kutta technique with Shooting method. Rajeswari et al. [25] employed the two dimensional flow due to a stretching surface in a viscoelastic fluid with effect of heat and mass transfer using analytical method.

An excellent review of heat transfer papers published during 1999 and 2002 are given by Goldstein et al. [8], [9] in which the heat transfer studies due to several flows in different types of geometries under various conditions are discussed very lucidly.

2. Problem Formulation and Governing Equation

Here we consider the steady laminar motion of a viscous, incompressible fluid caused by the stretching of a surface in an ambient fluid. The flat surface is coincident with the plane $y = 0$, and the flow is confined to the region $y > 0$. Two equal and opposite forces are applied along the x-axis so that the wall is stretched but the origin remains fixed. The surface is stretched with a velocity proportional to the distance x along the surface. The surface is assumed to have either power-law temperature distribution or power-law heat flux distribution. The fluid far away from the surface is kept at constant temperature.

The aim of the present study is to consider the effect of mass transfer, denoted by α (injection and suction) on the flow and heat transfer of a viscoelastic fluid over a continuous stretching surface placed in an ambient fluid. The effect of prescribed surface temperature or prescribed heat flux when the temperature has power law variation denoted by the parameter β is considered in the presence of source or sink parameter **s**. The governing partial differential equations have been reduced to a system of ordinary differential equations and an approximate analytical solution has been obtained using Homotopy Analysis Method.

The steady two dimensional boundary layer equations governing the flow are

$$u_x + v_y = 0, \tag{2.1}$$

$$uu_x + vu_y = \nu u_{yy} - \lambda_1 \left[(uu_{yy})_x + u_y v_{yy} + vu_{yyy} \right], \tag{2.2}$$

$$\rho C_p \left(uT_x + vT_y \right) = kT_{yy} + Q \left(T - T_\infty \right). \tag{2.3}$$

The boundary conditions for the problem when $x \geq 0$ are:

$$\begin{aligned} &u = Ax(A > 0),\ v = v_w,\ T = T_w \ \text{ or } \ -kT_y = q_w \text{ at } \ y = 0, \\ &u \to 0,\ T \to T_\infty \text{ as } y \to \infty. \end{aligned} \tag{2.4}$$

Since the problem is parabolic, the velocity u and the temperature T have to be prescribed at certain value of $x = x_0 (x_0 < 0)$ which are given by

$$u(x_0, y) = 0, \quad T(x_0, y) = T_\infty. \tag{2.5}$$

Here x and y are distances along and perpendicular to the surface, respectively; u and v are the components of the velocity along the x- and y- directions, respectively; T is the temperature; Q is the source or sink parameter; k is the thermal conductivity; λ is the viscoelastic parameters; ρ is the density; ν is the kinematic viscosity; C_p is the specific heat at a constant pressure; q_w is the surface heat flux; the subscripts w and ∞ denote conditions at the surface and in the free stream, respectively.

It may be remarked that the partial differential equations.(2.1)-(2.3) under conditions eq.(2.4) and eq.(2.5) admit similarity solutions when the surface velocity

$u_w = Ax(A > 0)$. We apply the following transformations

$$\eta = \left(\frac{A}{\nu}\right)^{1/2} y, \quad u = Axf'(\eta), \quad v = -(A\nu)^{1/2} f(\eta), \quad T - T_\infty = (T_w - T_\infty) g(\eta),$$
$$T_w - T_\infty = (T_{w_0} - T_\infty)\left(\frac{x}{L}\right)^\beta, \quad T - T_\infty = \left(\frac{q_{w_0}}{k}\right)\left(\frac{x}{L}\right)^\beta \left(\frac{\nu}{A}\right)^{1/2} G(\eta),$$
$$\lambda = \lambda_1 \frac{A}{\nu}, \quad q_w = q_{w_0}\left(\frac{x}{L}\right)^\beta, \quad Pr = \frac{sC_p}{k}, \quad s = \frac{Q\nu}{kA}, \quad \alpha = -\frac{(v)_w}{(A\nu)^{1/2}}, \tag{2.6}$$

to eqs.(2.1)-(2.3) and we find that eq.(2.1) is identically satisfied and eqs.(2.2) and (2.3) reduced to

$$f''' + ff'' - (f')^2 = \lambda[2f'f''' - (f'')^2 - ff''''], \tag{2.7}$$
$$g'' + Prfg' - (Pr\beta f' - s)g = 0 \qquad \text{(PST case)}, \tag{2.8}$$
$$G'' + PrfG' - (Pr\beta f' - s)G = 0 \qquad \text{(PHF case)}. \tag{2.9}$$

The boundary conditions eqs.(2.4) and (2.5) are rewritten as

$$f(0) = \alpha, \quad f'(0) = 1, \quad f'(\infty) = 0, \tag{2.10}$$
$$g(0) = 1, \quad g(\infty) = 0 \quad \text{(PST case)}, \tag{2.11}$$
$$G(\infty) = 0, \quad G'(0) = -1 \quad \text{(PHF case)}. \tag{2.12}$$

Here η is the similarity variable, f is the dimensionless stream function; f' is the dimensionless velocity; g and G are the dimensionless temperatures; Pr is the Prandtl number; L is the characteristic length; T_{w_0} and q_{w_0} are constants; β is the index in the power-law variation of wall temperature or heat flux; s is the dimensionless source or sink parameter; and prime denotes derivative with respect to η. α is the mass transfer parameter (α is a constant when v_w is a constant). Also $\alpha \lesseqgtr 0$ according to whether there is suction or injection. The heat transfer coefficient of in terms of Nusslet number is expressed as

$$Nu = -\frac{(T_y)_w\ x}{T_w - T_\infty} = -(Re_x)^{1/2} g'(0) \qquad \text{(PST case)},$$
$$Nu = \frac{(Re_x)^{\frac{1}{2}}}{G(0)} \qquad \text{(PHF case)}, \tag{2.13}$$

where $Re_x(= Ax^2/\nu)$ is the local Reynolds number.

3. HAM Analysis

The method of homotopy analysis is used for obtaining the approximate analytic solution. For the details the methods one can refer to first described in detail by Liao [12] as they are not presented here for the sake of brevity.

The main components of the HAM procedure are selecting suitable initial profiles satisfying the boundary conditions of the problem; choosing an appropriate linear operator so that its solutions are simpler to evaluate analytically. The nonlinear operator is directly written from the governing equation of the problem. In

Homotopy analysis, we always get a system of deformation equations which have to be solved. We choose the initial guesses and auxiliary linear operators as follows.

$$f_0(\eta) = \alpha + 1 - e^{-\eta}, \quad g_0(\eta) = e^{-\eta}, \quad G_0(\eta) = e^{-\eta}. \tag{3.1}$$

$$L_f = \frac{d^3 f}{d\eta^3} - \frac{df}{d\eta}, \quad L_g = \frac{d^2 g}{d\eta^2} - g, \quad L_G = \frac{d^2 G}{d\eta^2} - G, \tag{3.2}$$

so that

$$L_f\left[C_1 + C_2 e^{\eta} + C_3 e^{-\eta}\right] = 0, L_g\left[C_4 e^{\eta} + C_5 e^{-\eta}\right] = 0, L_G\left[C_6 e^{\eta} + C_7 e^{-\eta}\right] = 0, \tag{3.3}$$

in which C_i are arbitrary constants, these C_is can be obtained using the boundary conditions given in eqs.(2.10)-(2.12).

3.1. Higher-order deformation Equations

To obtain the HAM solution for the governing eqs.(2.7)-(2.9), let $\gamma \in [0, 1]$ be an embedding parameter and c_f, c_g and c_G are the basic convergence control parameters. Then the zeroth order deformation equation and the non-linear operators become,

$$(1-\gamma) L_X[X(\eta,\gamma) - X_0(\eta)] = \gamma c_X \mathcal{N}_X[X(\eta,\gamma)], \tag{3.4}$$

where, $X = f,\ g$ and G and $X_0 = f_0,\ g_0$ and G_0

$$\begin{aligned}\mathcal{N}_f[f(\eta,\gamma)] = {} & \frac{\partial^3 f(\eta,\gamma)}{\partial\eta^3} + f(\eta,\gamma)\frac{\partial^2 f(\eta,\gamma)}{\partial\eta^2} - \left(\frac{\partial f(\eta,\gamma)}{\partial\eta}\right)^2 \\ & - \lambda\left(2\frac{\partial f(\eta,\gamma)}{\partial\eta}\frac{\partial^3 f(\eta,\gamma)}{\partial\eta^3} - \left(\frac{\partial^2 f(\eta,\gamma)}{\partial^2\eta}\right)^2 - f(\eta,\gamma)\frac{\partial^4 f(\eta,\gamma)}{\partial\eta^4}\right),\end{aligned} \tag{3.5}$$

$$\begin{aligned}\mathcal{N}_g[g(\eta,\gamma), f(\eta,\gamma)] = {} & \frac{\partial^2 g(\eta,\gamma)}{\partial\eta^2} + Pr\left(f(\eta,\gamma)\frac{\partial g(\eta,\gamma)}{\partial\eta}\right) \\ & - g(\eta,\gamma)\left(Pr\beta\frac{\partial f(\eta,\gamma)}{\partial\eta} - s(\eta,\gamma)\right),\end{aligned} \tag{3.6}$$

$$\begin{aligned}\mathcal{N}_G[G(\eta,\gamma), f(\eta,\gamma)] = {} & \frac{\partial^2 G(\eta,\gamma)}{\partial\eta^2} + Pr\left(f(\eta,\gamma)\frac{\partial G(\eta,\gamma)}{\partial\eta}\right) \\ & - G(\eta,\gamma)\left(Pr\beta\frac{\partial f(\eta,\gamma)}{\partial\eta} - s(\eta,\gamma)\right),\end{aligned} \tag{3.7}$$

with appropriate boundary conditions given as in eqs. (2.10)-(2.12) we have,

$$f(\eta;\gamma)|_{\eta=0} = \alpha, \quad \left.\frac{\partial f(\eta;\gamma)}{\partial\eta}\right|_{\eta=0} = 1, \quad \left.\frac{\partial f(\eta;\gamma)}{\partial\eta}\right|_{\eta=\infty} = 0, \tag{3.8}$$

$$g(\eta;\gamma)|_{\eta=0} = 1, \quad g(\eta;\gamma)|_{\eta=\infty} = 0 \qquad \text{(PST case)}, \tag{3.9}$$

$$G(\eta;\gamma)|_{\eta=\infty} = 0, \quad \left.\frac{\partial G(\eta;\gamma)}{\partial\eta}\right|_{\eta=0} = -1 \quad \text{(PHF case)}. \tag{3.10}$$

For l^{th} -order deformations equations, we first differentiate eq.(3.4) in l-times with respect to γ, dividing them by $l!$ and then setting $\gamma = 0$. Following this we have,

$$L_X[X_l(\eta) - \Omega_l X_{l-1}(\eta)] = c_X \mathcal{R}_l^X(\eta), \tag{3.11}$$

where $X = f$, g and G, with its boundary conditions such as,

$$\begin{aligned} &f_l(0) = \alpha,\ f_l'(0) = 1,\ f_l'(\infty) = 0, \\ &g_l(0) = 1,\ g_l(\infty) = 0 \qquad \text{(PST case)}, \\ &G_l(\infty) = 0,\ G_l'(0) = -1 \qquad \text{(PHF case)}, \end{aligned} \tag{3.12}$$

where $\mathcal{R}_l^f(\eta)$, $\mathcal{R}_l^g(\eta)$ and $\mathcal{R}_l^G(\eta)$ are remained of linear operators such as,

$$\begin{aligned} \mathcal{R}_l^f(\eta) =& f_{l-1}'''(\eta) + \sum_{j=0}^{l-1}[f_{l-1-j}f_j'' - f_{l-1-j}'f_j'] \\ &- 2\lambda\sum_{j=0}^{l-1}[f_{l-1-j}'f_j''' + f_{l-1-j}''f_j'' + f_{l-1-j}f_j''''], \end{aligned} \tag{3.13}$$

$$\mathcal{R}_l^g(\eta) = g_{l-1}''(\eta) + Pr\sum_{j=0}^{l-1}[f_{l-1-j}g_j'] - \beta Pr\sum_{j=0}^{l-1}[f_{l-1-j}'g_j] + sg_{l-1}(\eta), \tag{3.14}$$

$$\mathcal{R}_l^G(\eta) = G_{l-1}''(\eta) + Pr\sum_{j=0}^{l-1}[f_{l-1-j}G_j'] - \beta Pr\sum_{j=0}^{l-1}[f_{l-1-j}'G_j] + sG_{l-1}(\eta), \tag{3.15}$$

where Ω_l defines as

$$\Omega_l = \begin{cases} 0 & \text{if } l \le 1, \\ 1 & \text{if } l > 1. \end{cases} \tag{3.16}$$

Expanding $X(\eta;\gamma)$ in Taylor's series with respect to γ we have

$$X(\eta;\gamma) = X_0(\eta) + \sum_{l=1}^{\infty} X_l(\eta)\gamma^l, \quad X_l(\eta) = \frac{1}{l!}\frac{\partial^l X(\eta;\gamma)}{\partial\gamma^l}\bigg|_{\gamma=0}. \tag{3.17}$$

The auxiliary parameters are selected as $\gamma = 0$ and $\gamma = 1$ from eq.(3.4), one may write

$$X(\eta;0) = X_0(\eta),\ X(\eta;1) = X(\eta). \tag{3.18}$$

Thus as γ increases from 0 to 1 and $X(\eta;\gamma)$ varies from the initial guess $X_0(\eta)$ to the solution $X(\eta)$ of the governing equations respectively. The auxiliary parameters are selected so that the series solutions converge for $\gamma = 1$ and the particular solution is

$$X(\eta) = X_0(\eta) + \sum_{l=1}^{\infty} X_l(\eta), \tag{3.19}$$

where $X = f^*$, g^* and G^*. Therefore, we get the general approximate analytical solutions $(f_l,\ g_l,\ G_l)$ in terms of special solutions $(f_l^*,\ g_l^*,\ G_l^*)$ are given by

$$f_l(\eta) = f_l^*(\eta) + C_1 + C_2e^{\eta} + C_3e^{-\eta}, \tag{3.20}$$

$$g_l(\eta) = g_l^*(\eta) + C_4e^{\eta} + C_5e^{-\eta}, \tag{3.21}$$

$$G_l(\eta) = G_l^*(\eta) + C_6e^{\eta} + C_7e^{-\eta}. \tag{3.22}$$

We solve the eqs.(3.20)-(3.22) one after the other in the order $l = 1, 2, 3, \ldots$ by means of the symbolic computation software Mathematica. It is shown that the solution for the velocity profile can expressed as an infinite series of any desired order.

4. Error estimation at High orders

An optimal value of the convergence control parameter c_0, integrated in the whole region $[0, \infty)$ have the exact squared residual error at l^{th}-order of approximation [17], [21] and [19], [4] are given by

$$\Delta_l = \int_0^{+\infty} \left(N \left[\sum_{i=0}^{l} X_i(\eta) \right] \right)^2 d\eta, \tag{4.1}$$

where $X = f$, g and G.

At every l^{th}-order of approximation, Δ_l takes at most three convergence control parametric values for eq.(3.20) and at most two for eq.(3.21) and (3.22). The convergence control parameters are represented by c_f, c_g and c_G for governing equations eqs.(2.7), (2.8) and eq.(2.9) respectively. When Δ_l decreases to zero rapidly then the homotopy series solutions converges faster.

In that case, at the l^{th}-order of approximation, the corresponding optimal values of the convergence control parameters are given by the minimum of Δ_l, for the coupled nonlinear algebraic equations as follows.

$$\frac{\partial \Delta_l}{\partial c_f} = 0; \quad \frac{\partial \Delta_l}{\partial c_g} = 0; \quad \frac{\partial \Delta_l}{\partial c_G} = 0 \tag{4.2}$$

Whenever, the eq.(3.19) is known to be convergent series, the eqs.(3.20)-(3.22) represent the exact solution of governing equations. But, eq.(4.1) requires too much CPU time to compute the exact residual errors even for the low order of approximation. It is observed that, it needs 42.31, 296.86 and 965.116 seconds of CPU time for $l = 2, 4$ and 6 respectively and therefore not very useful in practice.

To overcome this, we compute averaged residual errors suggested by [17]

$$E_X \simeq \frac{1}{l} \sum_{j=0}^{i} \left(N \left[\sum_{i=0}^{l} X_i(j\Delta x) \right] \right)^2, \tag{4.3}$$

where $\Delta x = \frac{10}{l}$ and $l = 20$ for the governing equations (2.7)-(2.9). The HAM-based **Mathematica package BVPh 2.0*** has been utilized to compute the averaged residual errors of eqs.(2.7)-(2.9). The exact squared residual error computed using eq.(4.1) and convergence control parameters(i.e, c_f, c_g and c_G) at the 10^{th}, 16^{th} and 20^{th}-order approximation are as shown in Figures.1-3. It is observed from computation that, the exact squared residual increases in the region of $c_f \in [-1.5, -0.9]$, decrease in the region of $c_g \in [-1.8, -1.0]$ and increases in the region of $c_G \in [-1.9, -0.6]$ as the order of approximation increases, which shows that the series solution converges for c_f, c_g and c_G at arbitrary values. The exact squared residual attains its minimum values at $c_f = -1.25846$, $c_g = -1.02823$ and $c_G = -1.0262$. These calculations, not only give the efficiency region of the convergence control parameters but also their appropriate values to enable faster convergence of the solution series. The same analysis has been carried out for averaged residual errors too using eq.(4.3).

Table-1 gives the minimum of the averaged squared residual errors for E_f, E_g and E_G for different orders of approximation. The minimum value of these averaged

*Ref. http://numericaltank.sjtu.edu.cn/BVPh.htm

Table 1. Minimum of the averaged squared residual error E_f, E_g and E_G with the CPU time at fixed $c_f = -1.25846$, $c_g = -1.02823$ and $c_G = -1.0262$.

l	Minimum of Averaged Squared Residual Errors			
	CPU time(Sec.)	E_f	E_g	E_G
2	0.22801	3.06471×10^{-7}	2.22635×10^{-7}	8.3716×10^{-7}
4	1.43008	1.82403×10^{-10}	1.26878×10^{-10}	2.49866×10^{-10}
6	4.01023	2.17438×10^{-13}	1.34723×10^{-11}	1.30498×10^{-11}
8	8.20247	4.06611×10^{-16}	1.42224×10^{-12}	2.82727×10^{-12}
10	13.8808	9.65429×10^{-19}	1.09374×10^{-16}	9.26369×10^{-16}
12	22.0793	2.60275×10^{-21}	1.16563×10^{-18}	1.26017×10^{-18}
14	32.2448	7.91939×10^{-24}	6.31826×10^{-20}	7.31169×10^{-20}
16	43.3805	2.75127×10^{-26}	5.07436×10^{-22}	1.25455×10^{-21}

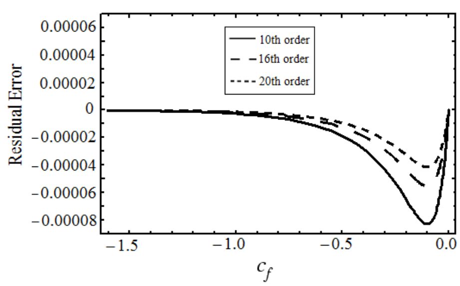

Figure 1. Exact residual error for the function $f(\eta)$.

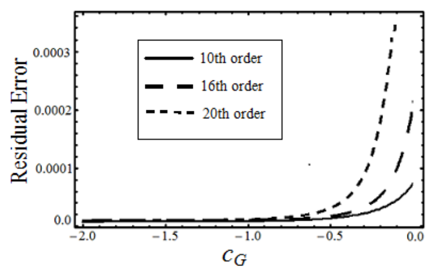

Figure 2. Exact residual error for the function $g(\eta)$.

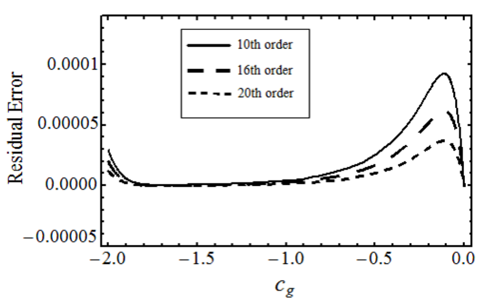

Figure 3. Exact residual error for the function $G(\eta)$.

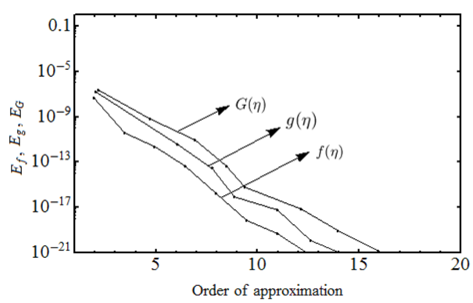

Figure 4. Averaged squared residual error at different order of approximations.

squared residuals for the computation of series solutions for f, g and G respectively are found to be $(E_f)_{l=10} = 9.65429 \times 10^{-19}$, $(E_g)_{l=14} = 6.31826 \times 10^{-20}$ and $(E_G)_{l=10} = 9.26369 \times 10^{-16}$ at $c_f = -1.25846$, $c_g = -1.02823$ and $c_G = -1.0262$.

In particular, for the case of $l \leq 6$, it takes only 0.228013, 1.43008 and 4.01023 seconds of computing time to get optimal convergence control values (using eq.(4.3)) for $l = 2, 4$ and 6 respectively. This is much much smaller compared to the CPU time needed to compute exact squared residual errors (using eq.(4.1)) for the same set of $l = 2, 4$ and 6 which are found to be 42.31, 296.86 and 965.116 seconds, respectively. Hence by using eq.(4.3) to calculate the squared residuals we use only 0.53% of CPU time for $l = 2$; 0.48% of CPU time for $l = 4$ and 0.41% of CPU time for $l = 6$ compared to exact squared residual computation using eq.(4.1). It is found that, the CPU time required to compute errors using eq.(4.3) is much less than that of using eq.(4.1). Hence, we use only eq.(4.3) to find the convergence control parameters for entire calculations.

The averaged squared residual at different orders of approximation for $f(\eta)$, $g(\eta)$ and $G(\eta)$ is shown as Fig.4. The corresponding averaged squared residual decreases much more quickly with convergence control parameters $c_f = -1.25846$, $c_g = -1.02823$ and $c_G = -1.0262$. Therefore, the suitable choice of convergence control parameter can greatly accelerate the convergence of series solution in HAM.

5. Results and Discussion

We have studied the effect of various parameters such as visco elastic parameter, mass transfer parameter, effect of source/sink in PST and PHF cases on velocity and temperature profiles as well as in skin friction and heat transfer rates. It is found that, velocity and temperature profiles increase, increasing visco elastic parameter and mass transfer parameter values. The heat transfer values decreases as the mass transfer parameter is raised. The effect is similar even for the increase in visco elastic parameters.

Table 2. Convergence of Homotopy solution for different orders of approximation for $-f''(0)$, $-g'(0)$ and $-G'(0)$ when ($\alpha = 0.1$, $\beta = 0.5$ and $s = 0.1$, $\lambda = 0.2$.)

l	$-f''(0)$	$-g'(0)$	$-G'(0)$
1	1.1280000	0.6750000	0.4055992
5	1.1998968	0.6139803	0.4115234
10	1.2014585	0.6012477	0.4115303
15	1.2014756	0.6012218	0.4115304
20	1.2014757	0.6012215	0.4115304
25	1.2014758	0.6012213	0.4115304
30	1.2014758	0.6012213	0.4115304
35	1.2014758	0.6012213	0.4115304

Computations have been carried out for velocity and temperature profiles and for skin friction coefficients and heat transfer rates for several combinations of parameters α, λ, β, s and only few important and interesting results are reported in this research article in the form of tables and figures.

Table-2 illustrates the convergence of skin friction $-f''(0)$, heat transfer $-g'(0)$ and $-G'(0)$ after performing up to 35^{th}-order approximation of functions f, g and G computed from deformation equations. As seen, the computation is terminated as soon as three consecutive values agree in their seventh decimal places. For the special case $\alpha = 0$ (in the absence of mass transfer), Table-3 shows the comparison of skin friction results with that of Prasad et al. [22] and found them to be in very good agreement.

Table 3. Comparison of Skin friction coefficients $-f''(0)$ for various values of viscoelastic parameter when ($\alpha = 0.0$, $\beta = 0.5$ and $s = 0.1$)

λ	$-f''(0)$	
	Prasad et al. [22]	Present
0.0	—	1.0000000
0.1	1.0663694	1.0658414
0.2	1.1113553	1.1116667
0.3	1.1909626	1.1904193
0.4	—	1.2773057
0.5	—	1.3798041

It is seen from Table-4 that the heat transfer rates for different Prandtl numbers (and for two different values of mass transfer) for a fixed $\beta = 3.0$ is compared in the absence of visco elastic parameter with that of Chen and Char [5]. It is found that the values of the heat transfer coefficients in terms of local Nusselt number are small for $Pr = 0.01$ in comparison to the values for $Pr = 1.0$. This means that the values of the local Nusselt number increases with an increase in Prandtl number.

Table 4. Comparison of heat transfer rates($-g'(0)$) for different Pr, when ($s = 0.0$, $\lambda = 0.0$ and $\beta = 3.0$.)

	$-g'(0)$			
Pr	Chen and Char [5]		Present	
	$\alpha = 0.7$	$\alpha = 2.0$	$\alpha = 0.7$	$\alpha = 2.0$
0.01	0.047667	0.034729	0.0474709	0.0347462
0.10	0.352134	0.326386	0.3519053	0.3261310
0.72	1.150099	1.854735	1.1508700	1.8546038
1.00	1.342679	2.429752	1.3421119	2.4266375

The effect of visco elastic parameter and mass transfer on velocity profiles are plotted in Figs.5 and 6. It is observed that there is a slight overshoot in velocity profiles as λ increases, but the increase in mass transfer parameter α makes the velocity profiles to converge faster to its free stream values.

The temperature variation for PST and for PHF cases by for different source/sink parameters are presented in Figs. 7 and 8. There is a temperature overshoot as s increases for both PST and PHF cases, but the values are higher for PST compared to PHF. The effect of heat transfer rates for the PST case, for various values of s are plotted in Fig. 9. It is found that the heat transfer rate is not affected much by the change in the power law index for a given value of s. However, the heat transfer rate increases as the source/sink parameter value increases for a given β. The variation of heat transfer rates versus β for various values of visco elastic parameter presented in Fig. 10 shows the increase in heat transfer rates for increase on λ as well as β.

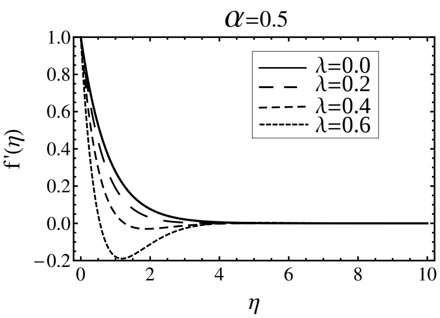

Figure 5. Effect of visco elastic parameter on velocity profiles.

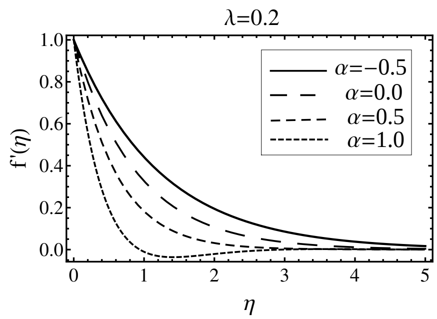

Figure 6. Effect of mass transfer (injection) on velocity profiles.

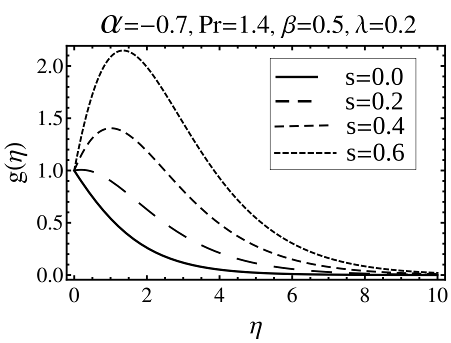

Figure 7. Effect of source/sink on temperature profiles (PST case).

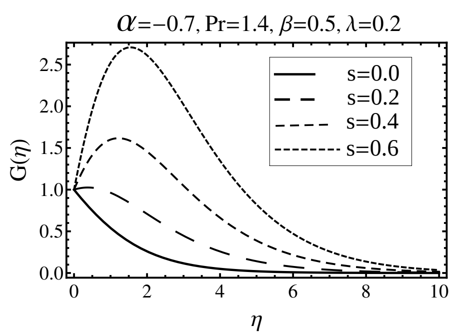

Figure 8. Effect of source/sink on temperature profiles (PHF case).

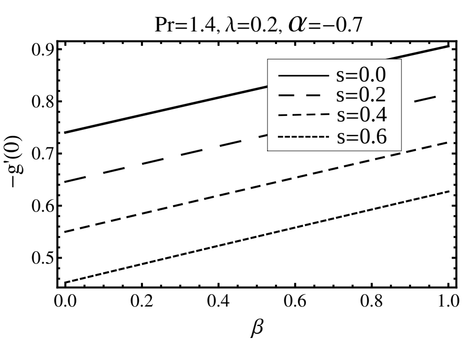

Figure 9. Effect of source/sink on heat transfer rate (PST case).

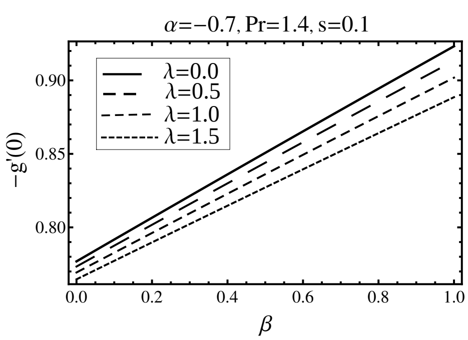

Figure 10. Effect of viscoelastic parameter on heat transfer rate (PST case).

Figs. 11 and 12 give the temperature profiles for the prescribed surface temperature(PST) and prescribed heat flux(PHF) cases for various values of mass transfer parameter. In the case of increasing values suction ($\alpha < 0$), the profiles tend to approach to the free stream values faster where as in the case of injection ($\alpha > 0$) there is a slight overshoot in the temperature profiles close to the wall and then it gradually approaches to free stream values.

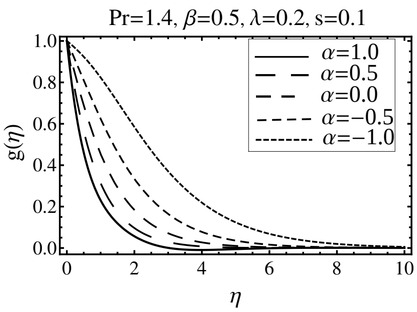

Figure 11. Effect of mass transfer parameter on temperature profiles (PST case).

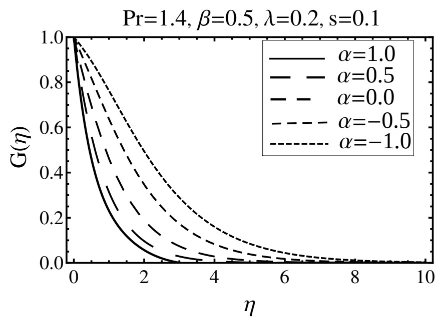

Figure 12. Effect of mass transfer parameter on temperature profiles (PHF case).

6. Conclusion

The flow, heat and mass transfer analysis is carried out on a viscoelastic fluid over a continuous stretching surface in an ambient fluid. Using Homotopy Analysis Method (HAM), a series solution in the form of polynomials are derived with the wall normal height η as a variable for velocity f and temperature g and G. The coefficients of the polynomial contain all the other parameters such as λ, β, s and α. The computations have been carried out to retain at least up to 20^{th} degree in η in the polynomial expressions of f, g and G to get the results accurate up to seventh decimal place. The Computer Algebra Software Mathematica is used to perform these semi-analytical calculations. The effect of various parameters such as mass transfer parameters α, viscoelastic parameters λ are studied on flow velocities. The influence of power law variation β on PST and PHF cases, the presence of source/sink parameter s and the effect of Prandtl number Pr on the temperature profiles and heat transfer rates are also analyzed. Thus the present study helps in identifying a suitable parameter that can be used to increase or decrease the heat transfer rates of the continuous moving surface thereby enhancing the final product to a desired characteristics. Visco elastic parameter, heat and mass transfer parameters helps in controlling the boundary layer thickness of both velocity and temperature.

The following conclusions are drawn from the present study.

- The velocity profiles decreases for the increase in λ and α values whereas the trend is quite opposite for the temperature profiles.
- The skin friction coefficients decreases for the increase in the values of visco elastic parameter for any fixed value of α.
- The temperature profiles increases for the increase in the values of mass transfer parameter and source/sink parameter where as it decreases for the increase in the values of power law index on temperature and Prandtl number.
- The heat transfer rates are almost nil when $\lambda = s = 0$. The heat transfer rates increases for the increase in α, β and Pr, but decreases for the increase

in λ and source/sink parameter. Another observation is that the heat transfer rates show similar trend for both PST and PHF cases for the change of all the parameters but the heat transfer values for PHF case is always at a lower value compared to that of PST case.

Acknowledgements

The authors express their sincere thanks to the referees for their valuable comments and suggestions that helped us to understand residual calculations better, which improved the results. The author S. Rao Munjam gratefully acknowledge UGC-Rajiv Gandhi National Fellowship(RGN-SRF), Government of India for providing financial assistance.

References

[1] S. Abbasbandy, *Applications of homotopy analysis method to nonlinear equations arising in heat transfer*, Physics Letters A., 360(2006), 109-113.

[2] M.S. Abel and N. Mahesha, *Heat transfer in MHD viscoelastic fluid flow over a stretching sheet with variable thermal conductivity, non-uniform heat source and radiation*, Applied Mathematical Modeling., 32(2008), 1965-1983.

[3] M.A.F. Araghi and S. Naghshband, *On Convergence of q-homotopy analysis method*, Int. J. Contep. Math. Sciences., 8(2013), 481-497.

[4] M.A.F. Araghi and S. Naghshband *On Convergence of homotopy analysis method to solve the schrodinger equation with a power Law nonlinearity*, Int. J. Industrial Mathematics., 5(2013), 1-8.

[5] C.K. Chen and M.I. Char, *Heat transfer of a continuous, stretching surface with suction or blowing*, Journal of Mathematical Analysis and Applications., 135(1988), 568-580.

[6] L.J. Crane, *Flow past a stretching plate*, Z. Angew. Math. Mech., 21(1970), 645-647.

[7] I.E. Erickson, L.T Fan and V.G. Fox *Heat and mass transfer on a moving continuous fast plate with suction or injection*, Ind.Engng Chem. Fundm., 5(1966), 19-25.

[8] R.J. Goldstein, E.R.G Eckert, W. E. Ibele, S.V Patankar, T.W. Simon, T.H Kuehn, P.J. Strykowski, K.K. Tamma, A. Bar Cohen, J.V.R. Heberlein, J.H. Davidson, J. Bischof, F.A. Kulacki, U. Kortshagen and S. Garrick, *Heat transfer-a review of 1999 literature*, International Journal of Heat and Mass Transfer., 44(2001), 3579-3699.

[9] R.J. Goldstein, E.R.G Eckert, W.E. Ibele, S.V Patankar, T.W. Simon, T.H Kuehn,P.J. Strykowski, K.K. Tamma, A. Bar Cohen, J.V.R. Heberlein, J.H. Davidson, J. Bischof, F.A. Kulacki, U. Kortshagen, S. Garrick and V. Srinivasan, *Heat transfer-a review of 2002 literature*, International Journal of Heat and Mass Transfer., 48(2005), 819-927.

[10] T. Hayat, S.A. Shehzad, and A. Alsaedi, *Soret and dufouf effects on MHD flow of casson fluid*, Appl. Math. Engl. Ed., 10(2012), 1301-1312.

[11] S.J. Liao, *A kind of approximate solution technique which does not depend upon small parameters(II): An application in fluid mechanics*, Int J. of Non-linear Mech., 32(1997), 815-822.

[12] S.J. Liao, *Beyond perturbation: Introduction to the homotopy analysis method*, CRC Press, Boca Raton: Chapman and Hall., (2003).

[13] S.J. Liao, *On the analytic solution of magnetohydrodynamic flows of non-newtonian fluids over a stretching sheet*, J. Fluid Mech., 488(2003), 189-212.

[14] S.J. Liao, *On the homotopy analysis method for nonlinear problems*, Applied Mathematics and Computation., 147(2004), 499-513.

[15] S.J. Liao, *Notes on the homotopy analysis method: Some definitions and theorems*, Commun Nonlinear Sci Numer Simulat., 14(2009), 983-997.

[16] S.J. Liao, *An optimal homotopy analysis approach for strongly nonlinear differential equations*, Commun Nonlinear Sci Numer Simulat., 15(2010), 2003-2016.

[17] S.J. Liao, *Homotopy analysis method in nonlinear differential equatuions*, Higher Education Press, Beijing., (2012).

[18] V. Marinca and N. Herisanu, *Applications of optimal homotopy asymptotic method for solving nonlinear equations arising in heat transfer*, Int. Communications in Heat and Mass Transfer., 35(2008), 710-715.

[19] K. Mallory and R.A. Van Gorder, *Control of error in the homotopy analysis of solutions to Zakharov system with dissipation*, Numer Algor., 64(2013), 633-657.

[20] J.C. Misra, G.C Shit and H.J. Rath, *Flow and heat transfer of a MHD viscoelastic fluid in a channel with stretching walls: Some applications to hemodynamics*, Computers and Fluids., 37(2010), 1-11.

[21] J.S. Nadjafi, R. Buzhabadi and H.S. Nik, *On the homotopy analysis method and optimal value of the convergence control parameter: Solution of Euler Lagrange equations*, Applied Mathematics., 3(2012), 873-881.

[22] K.V. Prasad, D. Pal, V. Umesh and N.S. Prasanna Rao, *The effect of variable viscosity on MHD viscoelastic fluid flow and heat transfer over a stretching sheet*, Communications in Nonlinear Science and Numerical Simulation., 15(2010), 331-344.

[23] B. Raftari and K. Vajravelu, *Homotopy analysis method for MHD viscoelastic fluid flow and heat transfer in a Channel with a stretching wall*, Commun Nonlinear Sci Numer Simulat., 10(2012), 4149-4162.

[24] S. Rajeswari, S. Nalini and G. Nath, *Viscoelastic fluid flow over a continuous stretching surface with mass transfer*, Mechanics Research Communications., 22(1995), 627-633.

[25] S. Rajeswari, S.R. Munjam and J. Sabaskar, *An analytical solution of heat transfer on a viscoelastic fluid over a continuous stretching surface*, Proceedings of the Indian Society of Theoretical and Applied Mechanics(ISTAM)., 2013.

[26] M. Sajid, Z. Iqbal, T. Hayat and S. Obaidat, *Series solution for rotating flow of an upper convected maxwell fluid over a stretching sheet*, Commun. Theor. Phys., 56(2011), 740-744.

[27] B.C. Sakiadis, *Boundary layer behavior on continuous solid surfaces: II. Boundary layer on a continuous flat surface*, AICHE Journal., 7(1961), 221-225.

[28] S.A. Shehzad, A. Alsaedi and T. Hayat, *Hydromagnetic steady flow of maxwell fluid over a bidirectional stretching surface with prescribed surface temperature and prescribed surface heat flux*, PLoS ONE., 8(2013), 1-10.

[29] S.A. Shehzad, T. Hayat, M. Qasim and S. Asghar, *Effects of mass transfer on MHD flow of Casson fluid with chemical reactio and suction*, Brazilian Journal of Chemical Engineering., 30(2013), 187-195.

[30] R.A. Van Gorder and K. Vajravelu, *On the selection of auxiliary functions, operators and convergence control parameters in the application of the homotopy analysis method to nonlinear differential equations: a general approach*, Commun. Nonlinear Sci. Numer. Simulat., 14(2009), 4078-4089.

[31] Y. Zhao, Z. Lin and S.J. Liao, *A modified homotopy analysis method for solving boundary layer equations*, Applied Mathematics., 4(2013), 11-15.